Neutron Diffraction Determination of Full Structures of Anhydrous Li–X and Li–Y Zeolites

C. FORANO,* R. C. T. SLADE,*,†,1 E. KROGH ANDERSEN,‡
I. G. KROGH ANDERSEN,‡ AND E. PRINCE†

*Department of Chemistry, University of Exeter, Exeter EX4 4QD, United Kingdom; †Reactor Radiation Division, National Institute of Standards and Technology, Gaithersburg, Maryland 20899; and ‡Department of Chemistry, Odense University, 5230 Odense M, Denmark

Virtually monoionic Li–X and Li–Y zeolites have been prepared by LiOH titration of parent NH_4 zeolites. Structural studies have been performed at room temperature on the anhydrous zeolites, $Li_{80.7}$ $H_{4.9}Na_{0.4}Al_{86}Si_{106}O_{384}$ and $Li_{46.0}H_{5.8}Na_{5.1}K_{0.1}Al_{57}Si_{135}O_{384}$, by powder neutron diffraction profile refinement in order to locate Li^+ cations. The cell parameters are 24.6716(10) and 24.4498(12) Å for Li–X and Li–Y, respectively. Three positions have been found for Li^+, sites I′ and II in the six-ring windows of the sodalite unit and site III′ in the supercage for the additional Li^+ of Li–X. © 1989 Academic Press, Inc.

1. Introduction

Anhydrous alkali metal X zeolites (type FAU) are ionic conductors. Recently, the ac conductivity of (Na, Li, K, Cs)–X zeolites has been measured in the temperature range from room temperature to ≈300°C (1). All the compounds display a reversible Arrhenius-type thermal activated behavior. Specific conductivities at 150°C are in the range from 5×10^{-10} ohm^{-1} cm^{-1} for the cesium form to 3×10^{-6} ohm^{-1} cm^{-1} for the sodium form. Below 150°C substitution of even small amounts of sodium ions with lithium ions decreases the conductivity by one order of magnitude or more and raises the activation energy. Above 360°C Li–X has a conductivity higher than that of Na–X. The unit cell framework $[Al_x$

$Si_{192-x}O_{384}]^{x-}$ of the zeolites X and Y (labeled as $M_y - Z[x]$ where y (if given) is the number of cations M in zeolite type Z with x aluminum per unit cell; $x = 74–96$ for Li–X and $x = 48–74$ for Li–Y) can be described as an arrangement of eight cuboctahedral sodalite units linked together tetrahedrally by 16 hexagonal prisms. This framework displays very large channels and cavities, the diameter of the supercage and the sodalite cage being 12–13 and 6–7 Å, respectively, very much larger than the ionic diameters of the alkali ions. Therefore the interaction between the cations and the anionic lattice is more important than the geometrical constraints in determining the location of exchangeable cations. In order to examine links between cationic positions and conductivity more structural information on virtually monoionic zeolites is necessary.

[1] To whom correspondence should be addressed at Exeter.

Monoionic Li zeolites are difficult to prepare (2, 3). By direct ion exchange of Na–X with 1.8 M lithium chloride solutions at 100°C Krogh Andersen et al. (1) obtained 89% exchange. The remaining cations were 6% "hydrogen ions" and 5% sodium ions. By a similar procedure but at 92°C Herden et al. (4) achieved 81% exchange. Full exchange for Y zeolites is usually found even more difficult to obtain. Subramanian et al. (5) obtained only 78.0% of Li exchange for Na–Y[56]. Franklin et al. (6) report that all sodium can be removed from Na–X by ion exchange with ammonium salts. The removal of sodium from Na–Y's is incomplete. In Na–Y[54] 87% of the sodium can be replaced by ammonium and in Na–Y[60] 94%. By the method described below 94 and 89 mol% exchange with ammonium in Na–X[86] and Na–Y[57], respectively, was obtained. The sodium ions were more completely exchanged in zeolite X (0.4% remains) than in zeolite Y (8.9% remains); a hydrogen ion exchange seems unavoidable for both compounds. The compositions of these materials in the hydrated state are $Li_{80.7}$ $H_{4.9}Na_{0.4}Al_{86}Si_{106}O_{384} \cdot 242H_2O$ and $Li_{46.0}$ $H_{5.8}Na_{5.1}K_{0.1}Al_{57}Si_{135}O_{384} \cdot 246H_2O$ for Li–X and Li–Y, respectively.

Herden et al. (7) determined the structure of the dehydrated Li–X and Li–Y with the respective compositions $Li_{64.8}H_{10.4}$ $Na_{10.8}Al_{86}Si_{106}O_{384} \cdot 270H_2O$ and $Li_{39.2}H_4$ $Na_{12.8}Al_{56}Si_{136}O_{384} \cdot 263H_2O$ (in the hydrated state) by X-ray powder diffractometry. Determination of Li ion positions by X-ray powder diffractometry is difficult. Moreover, only 130 of the 238 (i.e., 54.62%) and 78 of the 206 (i.e., 37.86%) electrons associated with the extra framework cations per unit cell come from lithium ions in the compounds X and Y investigated by Herden et al. (7). A powder neutron diffraction study (a more suitable technique to locate such light atoms (8, 9)) has therefore been carried out on both anhydrous zeolites

prepared in this work. In this paper the lithium ion positions and occupancies at room temperature are reported.

2. Experimental

2.1. Synthesis

The preparation of virtually monoionic Li–X zeolite was as follows. The starting material was the ammonium X zeolite with the composition $H_{13.4}(NH_4)_{72.3}Na_{0.63}Al_{86}$ $Si_{106}O_{384} \cdot 302H_2O$ prepared by stirring Na–X (Laporte) with 1 M NH$_4$Cl at room temperature. After 20 hr the solid was allowed to settle and the supernatant liquid was removed before a fresh solution was added. This procedure was repeated 37 times. A dispersion of 5 g NH$_4$ zeolite in 25 ml 2 M LiCl solution was titrated potentiometrically with 1 M LiOH solution. The titration was performed with an ABU 80 autoburette. The measuring electrodes were a glass electrode and a calomel/saturated ammonium chloride electrode. The calomel electrode was connected to the titration vessel through a salt bridge containing 2 M LiCl solution. The end point of the titration was set to pH 9.5. The ammonia was removed by bubbling nitrogen through the titration slurry. The titration was continued until release of ammonia stopped. The complete titration took 30 days. When the titration was nearly finished, IR spectra of the solid material were taken several times to check the removal of ammonium ions. The titration was stopped when the 1400-cm^{-1} IR band for ammonium was absent.

The starting material for preparing Li–Y was NH$_4$–Y with the composition $H_{4.2}$ $(NH_4)_{47.4}Na_{5.3}K_{0.2}Al_{57}Si_{135}O_{384} \cdot 195H_2O$ made by ion exchange of Na–Y (Laporte) by the same method as that described for NH$_4$–X, except that the ammonium chloride solution was renewed 49 times. A dispersion of 5 g NH$_4$–Y in 25 ml LiCl was titrated with 1 M LiOH solution as described above.

The alkali metal contents were determined by flame photometry after decomposition of the silicate by the method described by Langmyhr et al. (10).

The dehydrated materials were prepared by slowly heating hydrates to 250°C under vacuum overnight, heating for one day at 350°C and then quenching.

2.2. Diffraction Measurements

The two diffraction profiles were collected at the National Institute of Standards and Technology (NIST) research reactor on the five-detector neutron diffractometer BT-1, using a monochromatic beam at the wavelengths 1.5480 and 1.5454 Å for Li-X and Li-Y, respectively. Data were obtained at room temperature for the angle range $5° \leq 2\theta \leq 112°$ at increments of 0.05°.

The scattering length of the tetrahedral atom of the framework has been calculated from a linear combination of the scattering lengths of Al and Si, according to the Si/Al ratio for each zeolite (i.e., $b = 3.835 \times 10^{-15}$ and 3.940×10^{-15} m for Li-Y and Li-X, respectively). The values of 5.830×10^{-15} and -2.030×10^{-15} m were taken for the respective scattering lengths of O and Li.

The intensity profiles were fitted using a version of the Rietveld method program (11, 12) adapted to a five-detector system. A linear background was taken for each of the five detectors. At low angles, the curvature of the Debye–Scherrer ring within the height of the observing slit introduced an exaggerated asymmetry of the (111) Bragg reflexion which arises at 6–6.5°. The 5–8° data range was therefore omitted from the refinement (below).

2.3. Refinement of the Structure

Zeolites X and Y have the same structure as the mineral faujasite. All the Bragg reflections in both neutron powder patterns are indexed in the cubic $Fd3m$ space group.

The conventional origin at the 16c site was taken.

The first step of the refinement involved the location of the framework atoms (Al, Si), O_1, O_2, O_3, O_4, in the same sites previously found in faujasite (13). The labeling of the oxygen atoms conforms to Mortier's convention (14). At this stage, all the positional, background, unit cell, and zero point parameters, and the scale and thermal factors converged. The R values obtained for the two zeolites are already low (R_{wp} = 11.11% for Li-X and R_{wp} = 8.86% for Li-Y).

In a second step, the Li atoms were located. The different possible sites in which the exchangeable cations are usually expected and found (15–17) were tried: the octahedral site I in the center of the hexagonal prism, the trigonal sites I' and II' inside the sodalite unit, and the trigonal site II outside the sodalite unit in the supercage (Fig. 1). Difference Fourier maps were calculated using the anionic framework. Negative intensity peaks corresponding to Li atoms were found at two different positions $x = y = z \simeq 0.0333$ and $x = y = z \simeq 0.2167$ for Li-X, and $x = y = z \simeq 0.0406$ and $x = y = z \simeq 0.2190$ for Li-Y. Only for these two positions (32e sites) did the positional parameters converge with a meaningful improvement of the refinement. At this stage,
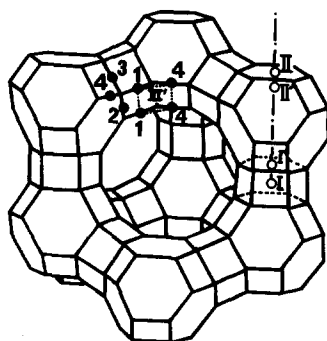

FIG. 1. Faujasite framework and cation sites following Mortier et al. (18).

refinement of the thermal and the occupancy factors for Li atoms gave the final fit for Li–Y (Table I).

In the case Li–X, the occupancy factor of Li$^+$ in site II refined to give a fully occupied site and this parameter was therefore constrained during subsequent refinements. The location of 26.24 Li in I' and 32 Li in II leaves 22.49 Li per unit cell to be located. The 12-ring region which constitutes the walls of the supercage was then investigated, and more especially the special positions 96h (x, $\bar{x}$, 0) and 96g (x, x, z) where Na$^+$ has been found respectively in the natural Na–faujasite (15) and in an hydrated synthetic zeolite Na$_{59}$–Y[57] (17). The investigation of all possibilities led to the

choice of the 96g site with $x = y = 0.092$ and $z = 0.893$ which yields the lowest R factor (Table I). The total numbers of Li atoms located are very close to the numbers determined by chemical analysis (99.2 and 98.3% of analytical value for X and Y, respectively); i.e., all Li has been located. It follows from the conductivity study that the populations of Li$^+$ determined are those at ambient temperature, facile change in site occupancy occurring with change in temperature.

Attempts to locate the five atoms of Na per unit cell in Li–Y in different sites of type I, I', or III' were unsuccessful. Convergent refinement of atomic position and occupancy factors was obtained for site II

TABLE I

FINAL REFINED PARAMETERS OF Li–X AND Li–Y ZEOLITES

Atom	Site		x	y	z	B (Å^2)	Occupancy factor
Tet^a	192i	X	0.1242(4)	0.9495(3)	0.0378(4)	1.02(13)	1.000
		Y	0.1240(4)	0.9495(4)	0.0358(4)	0.47(12)	1.000
O$_1$	96h	X	0.1014(2)	0.8986(3)	0.0000	2.69(27)	0.500
		Y	0.1021(3)	0.8979(3)	0.0000	2.10(30)	0.500
O$_2$	96g	X	0.2505(3)	0.2505(3)	0.1518(4)	2.03(21)	0.500
		Y	0.2511(3)	0.2511(3)	0.1493(5)	2.36(27)	0.500
O$_3$	96g	X	0.1780(3)	0.1780(3)	0.9787(3)	1.73(19)	0.500
		Y	0.1783(3)	0.1783(3)	0.9768(4)	1.47(22)	0.500
O$_4$	96g	X	0.1712(3)	0.1712(3)	0.3235(4)	1.47(22)	0.500
		Y	0.1733(3)	0.1733(3)	0.3218(5)	1.03(23)	0.500
Li I'	32e	X	0.0462(11)	0.0462(11)	0.0462(11)	1.87(1.23)	0.137(12)
		Y	0.0460(15)	0.0460(15)	0.0460(15)	2.67(1.79)	0.127(15)
Li II	32e	X	0.2220(13)	0.2220(13)	0.2220(13)	4.70(1.25)	0.167
		Y	0.2209(17)	0.2209(17)	0.2209(17)	2.36(1.97)	0.112(15)
Li III'	96g	X	0.0926(22)	0.0926(22)	0.8932(33)	0.77(1.87)	0.117(12)

	a (Å)	R_1(%)	R_p(%)	R_{wp}(%)	R_{exp}(%)
Li–X	24.6716(10)	10.24	7.95	10.16	9.41
Li–Y	24.4498(12)	9.76	6.69	8.53	7.66

^{a} (Si, Al) positions.

$$R_I = \frac{\Sigma|I_{obs} - I_{calc}|}{\Sigma I_{obs}}, \; R_p = \frac{\Sigma|Y_{obs} - Y_{calc}|}{\Sigma Y_{obs}}, \; R_{wp} = \sqrt{\frac{\Sigma w[Y_{obs} - Y_{calc}]^2}{\Sigma w[Y_{obs}]^2}}, \; R_{exp} = \sqrt{\frac{N - P + C}{\Sigma w[Y_{obs}]^2}}$$

and

$N - P + C$ = number of observations − number of variables + number of constraints.

($x = y = z = 0.2460$) but the thermal factor reached the high value of $B = 9.71$ Å^2, which is unsatisfactory. Na sites therefore remain unknown, and a mixed site occupancy (both Li$^+$ and Na$^+$) is not confirmed, although previously suggested for Li$_{39.2}$ Na$_{12.8}$–Y[56] (Herden (7)).

Attempts to refine using anisotropic thermal factors did not lead to any new information.

Figure 2 shows the refined powder neutron diffractograms of Li–X and Li–Y for all five detectors as well as the respective difference plots between the observed and calculated profiles. The atomic parameters for Li–X and Li–Y are given in Table 1. Bond lengths and bond angles are summarized in Tables II and III.

TABLE II

INTERATOMIC DISTANCES (Å)

		Li–X	Li–Y
Tet–O$_1$	(×1)	1.662(10)	1.628(11)
Tet–O$_2$	(×1)	1.696(9)	1.630(10)
Tet–O$_3$	(×1)	1.700(10)	1.688(10)
Tet–O$_4$	(×1)	1.640(10)	1.650(11)
Mean		1.674(10)	1.649(11)
O$_1$–O$_1$	(×2)	3.539(15)	3.531(10)
O$_1$–O$_2$	(×2)	2.784(7)	2.727(9)
O$_1$–O$_3$	(×2)	2.753(10)	2.712(11)
O$_1$–O$_4$	(×2)	2.686(4)	2.663(4)
O$_2$–O$_2$	(×2)	3.442(16)	3.444(20)
O$_2$–O$_3$	(×2)	2.709(8)	2.657(10)
O$_2$–O$_4$	(×2)	2.702(8)	2.636(10)
O$_3$–O$_3$	(×2)	3.258(15)	3.283(17)
O$_3$–O$_4$	(×2)	2.754(10)	2.755(10)
O$_4$–O$_4$	(×1)	3.222(19)	3.346(22)
LiI′–Tet	(×6)	3.073(10)	3.043(11)
LiI′–O$_2$	(×3)	3.073(9)	3.005(16)
LiI′–O$_3$	(×3)	1.894(9)	1.912(16)
LiII–Tet	(×6)	3.103(11)	3.070(11)
LiII–O$_2$	(×3)	1.996(10)	2.037(12)
LiII–O$_4$	(×3)	3.069(10)	2.966(11)
LiIII′–O$_1$	(×2)	2.298(56)	
LiIII′–O$_4$	(×2)	2.132(47)	
LiIII′–O$_3$	(×1)	2.222(75)	

TABLE III

BOND ANGLES (°)

	Li–X	Li–Y
O$_1$–Tet–O$_2$	111.9(6)	113.7(8)
O$_1$–Tet–O$_3$	110.0(7)	109.7(8)
O$_1$–Tet–O$_4$	108.9(7)	108.7(8)
O$_2$–Tet–O$_3$	105.8(6)	106.4(8)
O$_2$–Tet–O$_4$	108.2(8)	107.0(8)
O$_3$–Tet–O$_4$	112.0(7)	111.3(8)
Tet–O$_1$–Tet	145.7(9)	143.1(1.0)
Tet–O$_2$–Tet	130.4(8)	132.5(1.0)
Tet–O$_3$–Tet	125.0(7)	129.2(8)
Tet–O$_4$–Tet	138.8(1.0)	141.7(1.1)
O$_3$–LiI′–O$_3$	118.6(6)	118.3(8)
O$_2$–LiI′–O$_2$	119.7(2)	119.8(2)
O$_3$–LiI′–O$_2$	60.7(1)	60.7(1)
O$_2$–LiII–O$_2$	119.1(5)	118.3(8)
O$_4$–LiII–O$_4$	120.0(1)	119.9(1)
O$_2$–LiII–O$_4$	60.1(1)	60.2(1)
O$_4$–LiIII′–O$_4$	98.2(2.9)	
O$_1$–LiIII′–O$_1$	100.7(2.8)	
O$_1$–LiIII′–O$_4$	153.9(3.8)	
O$_3$–LiIII′–O$_4$	79.0(2.2)	
O$_3$–LiIII′–O$_1$	75.0(2.0)	

3. Discussion

The larger value of the cell parameter for Li–X arises from the higher Al-content in zeolite X[86] compared to zeolite Y[57]. Al exhibits a covalent radius (0.53 Å) greater than that of Si (0.40 Å) (20). For a zeolite with Si/Al $= n$ and a complete Si/Al disorder the calculated Tet–O distance should be approximately

Tet–O$_{calc} = (n \times 1.62 + 1.74)(1 + n)^{-1}$,

where 1.62 and 1.74 are the distances Si–O and Al–O (in Å) according to Shannon and Prewitt (20). The average Tet–O distances (Table II) are very close to the predicted ones (i.e., 1.673 and 1.655 Å for Li–X [86] and Li–Y [57], respectively). Both frameworks display regular tetrahedra with O–Tet–O angles near the theoretical value of 109°28′, the maximum deviation being less
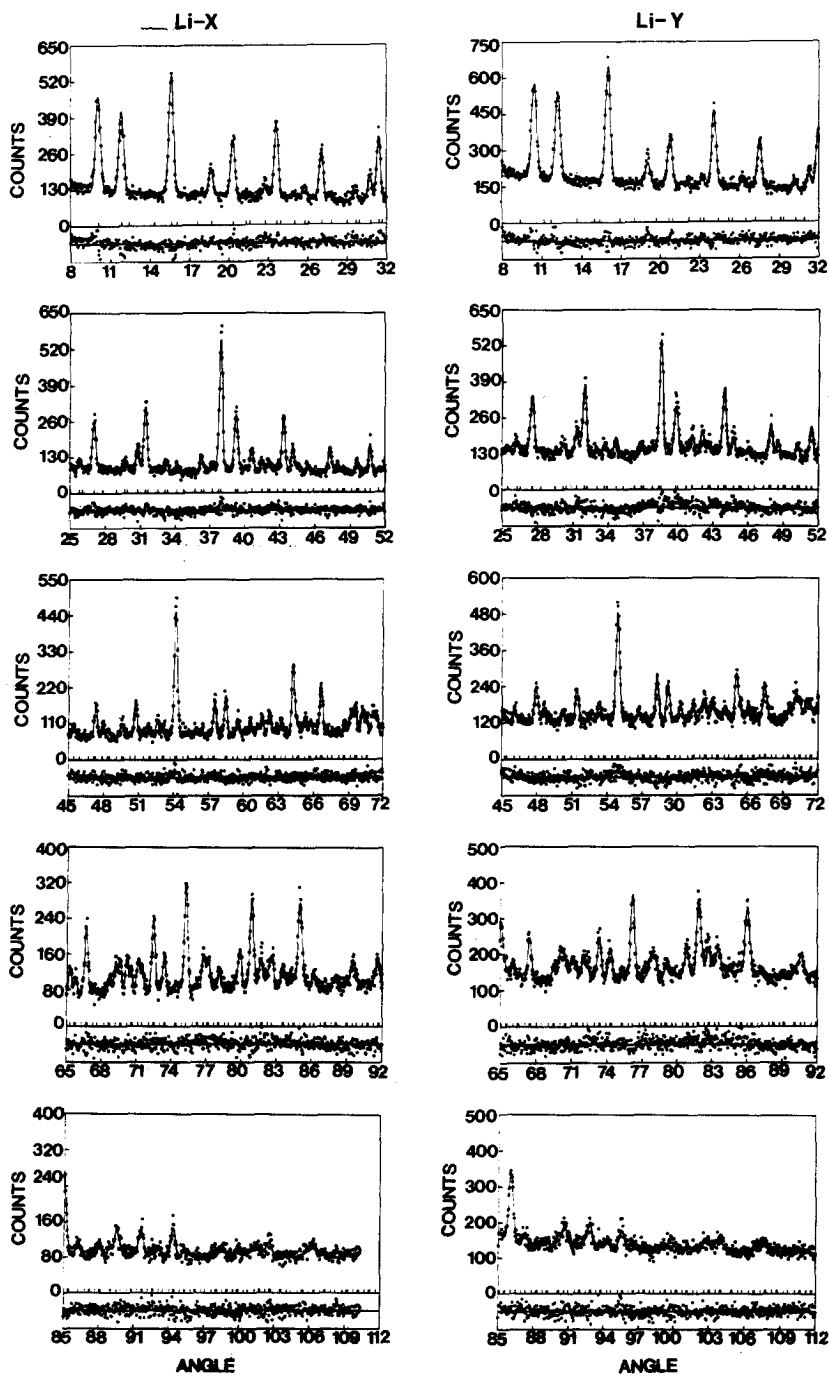
FORANO ET AL.

FIG. 2. Observed, calculated, and difference diffraction profiles for Li–X and Li–Y zeolites at room temperature.

than 4°41'. The Tet–O–Tet angles are in the usual range from 125° to 145°.

The major difference between the two frameworks is the contraction of the Li–Y hexagonal prism, which is evident in shortening of the Tet–O_n (n = 1, 2, 3) distances while the Tet–O_4 length, inside the sodalite cage, remains nearly the same for both zeolites. This is similarly confirmed by the decrease of the Tet–O_1–Tet angle.

The small differences in framework do not affect the geometry of the Li coordination for which the trigonal oxygen environments remain the same, the distances O_2–O_2 and O_3–O_3 being almost equal in both zeolites (Table II). Both Li in sites I' and II lie close to the central position of an equilateral triangle with O–Li–O angles close to 120°. A 0.1-Å lengthening of Li–O distance in the site II comes from the lack of stereochemical constraint on this window compared to that on the site I' window. The Li(I')–O distances are slightly smaller than the ones found in Li–A(BW) (21) and in bikitaite (22) (1.965 and 1.974 Å, respectively), where the Li ions have a tetrahedral coordination, but they are close to the bond distances found by Herden *et al.* (7) (as well as to the Li(II)–O distances). Site I is not occupied by the cation, in contrast to other anhydrous alkali metal zeolites X and Y (Table IV). The nearly regular octahedra environment (O_3-site(I)–O_3 ≃ 88° for both zeolites) of the six O_3 led to too long a distance site(I)–O_3 (2.34 Å for Li–X and 2.36 Å for Li–Y) to allow sufficient interactions between the framework oxygens and the small cation Li^+. Na^+ has been found by others in site I with six long site(I)–O_3 distances equal to 2.718(3) Å (23). Smaller Li^+ is found in I' and II within the sodalite unit, where shorter distances are allowed.

Li faujasite-type zeolites show a variation with cation content of the cation distribution between sites different to that in other alkali metal X and Y zeolites (Table IV). In the cases of the analogous Na and K zeolites decreasing the cation content affects the total population of sites I + I', while site II remains little affected. For Li zeolites, the population of site II is more affected than the occupancy of site I' where Li–oxygen interactions are stronger due to the shorter Li–O distances (1.894(9) and 1.912(16) Å for Li–X and Li–Y, respectively).

Very few cases (17) of anhydrous faujasite-type zeolites are known where the cation is definitively located in the 12-O-ring region of the supercage. This is the first

TABLE IV

OCCUPANCY OF SITES FOR Li, Na, AND K IN ANHYDROUS FAUJASITE-TYPE ZEOLITES

| Zeolites | Site type (symmetry) | | | | | Missing atoms | a (Å) | Ref. |
	I ($\bar{3}m$)	I' ($3m$)	II ($3m$)	III' (m)	M^a (m)			
$Li_{80.7}$[86]	—	26.3	32.0	22.4	—	—	24.67	(This work)
$Li_{64.8}$[86]	—	32.0	32.0	—	—	0.8	24.71	(6)
Li_{46} [57]	—	24.4	21.0	—	—	0.1	24.44	(This work)
$Li_{39.2}$[56]	—	32.0	7.2	—	—	—	24.59	(6)
Na_{81} [81]	3.8	32.3	30.8	—	7.9	6.2	24.92	(22)
Na_{57} [57]	7.7	19.5	30.3	—	—	—	24.71	(13)
K_{87} [87]	9.2	13.6	25.6	—	—	38.6	25.08	(14)
K_{55} [55]	5.4	18.1	26.8	—	—	4.7	24.82	(14)

^{a} The site M is a trigonal site with 2×3.1 Å Na–O_1 and 1×3.2 Å Na–O_2 distances (15).
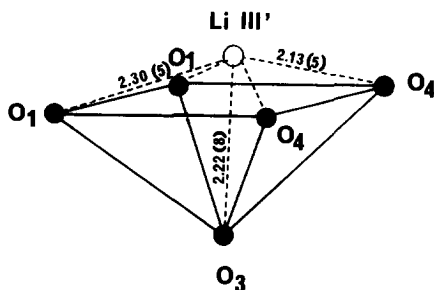
FIG. 3. Coordination of Li in site III'.

work which reports such a position for the small Li^+ cation. Li lies just above the base of a tetragonal pyramid formed by $2O_4$, $2O_1$, $1O_3$ (Fig. 3). The O_1–O_1 bond length (3.539 Å) is larger than the O_4–O_4 distance (3.222 Å), yielding a distortion of the pyramid (a slight shift of the Li toward the O_4–O_4 line). The Li–O_1 distance is of the same order as that in Li_8Na_4–A[12] (2.30 Å) (25).

Acknowledgments

References

1. E. KROGH ANDERSEN, I. G. KROGH ANDERSEN, J. METCALF-JOHANSEN, K. E. SIMONSEN, AND E. SKOU, Solid State Ionics 28–30, 249 (1988).
2. V. DONDUR AND R. DIMITRIJEVIC, J. Solid State Chem. 63, 46 (1986).
3. M. T. MELCHIOR, D. E. W. VAUGHAN, A. J. JACOBSON, AND C. F. PICTROSKI, "Proceedings, Sixth International Zeolites Conference" (D. Olson and A. Bisio, Eds.), p. 684, Butterworths, Surrey (1984).
4. H. HERDEN, D. HOPPACH, W.-D. EINICKE, R. SCHOLLNER, AND A. DYER, Z. Chem. 20, 272 (1980).
5. M. A. SUBRAMANIAN, D. R. CORBIN, AND R. D. FARLEE, Mater. Res. Bull. 21, 1525 (1986).
6. K. R. FRANKLIN, R. P. TOWNSEND, S. J. WHELAN, AND C. J. ADAMS, "Proceedings, 7th International Zeolite Conference" (Y. Murakami, A. Iijima, and J. W. Ward, Eds.), p. 289 (1986).
7. H. HERDEN, W.-D. EINICKE, R. SCHOLLNER, W. J. MORTIER, L. R. GELLENS, AND J. B. UYTTERHOEVEN, Zeolites 2, 131 (1982).
8. J. M. NEWSAM, "Proceedings, International Symposium on Neutron Scattering" (T. J. Hicks and T. M. Sabine, Eds.), Material Science Forum, Sydney (1987).
9. J. M. NEWSAM AND D. E. W. VAUGHAN, Zeolites 5, 239 (1985).
10. F. I. LANGMYHR AND P. E. PAUS, Anal. Chim. Acta, 397 (1968).
11. H. M. RIETVELD, J. Appl. Crystallogr. 2, 65 (1969).
12. E. PRINCE, "NBS Tech Note 1117" (F. Shorten, Ed.), p. 8 (1980).
13. G. R. EULENBERGER, D. P. SCHOEMAKER, AND J. G. KEIL, J. Phys. Chem. 71, 1812 (1967).
14. W. J. MORTIER, H. J. BOSMANS, AND J. B. UYTTERHOEVEN, J. Phys. Chem. 76, 650 (1972).
15. J. V. SMITH, "Zeolite Chemistry and Catalysis" (J. A. Rabo, Ed.), American Chemical Society, Washington, DC (1976).
16. R. M. BARRER, "Zeolites and Clays Minerals as Sorbents and Molecular Sieves," Academic Press, London (1978).
17. W. J. MORTIER, "Compilation of Extra Framework Sites in Zeolites," issued by the Structure Commission of the International Zeolite Association (1981).
18. W. J. MORTIER AND H. J. BOSMANS, J. Phys. Chem. 75, 3327 (1971).
19. J. MARTI, J. SORIA, AND F. H. CANO, J. Colloid Interface Sci. 40, 82 (1977).
20. R. D. SHANON AND C. T. PREWITT, Acta Crystallogr. Sect. B 25, 925 (1969).
21. E. KROGH ANDERSEN AND G. PLOUG-SORENSEN, Z. Kristallogr. 176, 67 (1986).
22. G. BISSERT AND F. LIEBAU, Neues Jahrb. Miner. Mh., 241 (1986).
23. A. N. FITCH, H. JOBIC, AND A. RENOUPREZ, J. Phys. Chem. 90, 1311 (1986).
24. T. HSEU, PhD thesis, University of Washington, University Microfilms No. 73-13835, Ann Arbor, MI (1972).
25. T. B. REED AND D. W. BRECK, J. Amer. Chem. Soc. 78, 5972 (1956).